2-D Mxene flakes as potential replacement for both TCO and Ptlayers for Dye-SensitizedSolar Cell

[a*]Muhammad Shakeel Ahmad, [b*]A.K. Pandey, [a]NasrudinAbd Rahim, [c]NavidAslfattahi,[d]Yogendra Kumar Mishra,[e]Bushra Rashid, [b,f]R. Saidur

[a]Higher Institution Centre of Excellence (HICoE), UM Power Energy Dedicated Advanced Centre (UMPEDAC), Level 4, Wisma R&D, University of Malaya, JalanPantai Baharu, 59990 Kuala Lumpur, Malaysia
[b]Research Center for Nano-Materials and Energy Technology (RCNMET), School of Engineering and Technology, Sunway University, Bandar Sunway, Petaling Jaya, 47500 Selangor, Darul Ehsan, Malaysia
[c]Department of Mechanical Engineering, Faculty of Engineering, University of Malaya, 50603 Kuala Lumpur, Malaysia
[d]Mads Clausen Institute, NanoSYD, University of Southern Denmark, Alsion 2, Sønderborg, DK- 6400 Denmark
[e]Faculty of Defence Science and Technology, National Defence University of Malaysia, 57000 Kuala Lumpur, Malaysia
[f]Department of Engineering, Lancaster University, Lancaster, LA1 4YW, UK

*Corresponding author(s):shakeelalpha@gmail.com (Muhammad Shakeel Ahmad);adarshp@sunway.edu.my ;adarsh.889@gmail.com (A. K. Pandey)

Abstract

The counter electrode (CE) containing catalyst layer and transparent conducting oxide (TCO) layer is by far the most expensive components in Dye sensitized solar cells (DSSC) due to use of rare earth element such as Pt. The potential replacement of both the TCO layer and Pt-based catalyst would essentially pave the way to mass commercialization of the technology of DSSC. In this investigation, an attempt has been made to replace both TCO and Pt with a single layer of delaminated 2-D MXene (Ti_3C_2) being produced by the leaching method which acted as both conducting layer and catalyst.Furthermore, the thickness of Ti_3C_2 has been optimized for maximum conversion efficiency. The TCO-Pt-free MXene based CEat optimum thickness exhibited a remarkable 8.68% conversion efficiency outperforming the standard TCO-Pt-based CE by 4.03%. The highefficiency is due to high conductivity, high available catalytic cites due to delaminated structure, and good catalytic activity of Ti_3C_2 towards iodide/triiodide electrolyte.

Keywords: Catalytic activity; Counter electrode; DSSC; MXene; TCO-Pt-free

Graphical Abstract

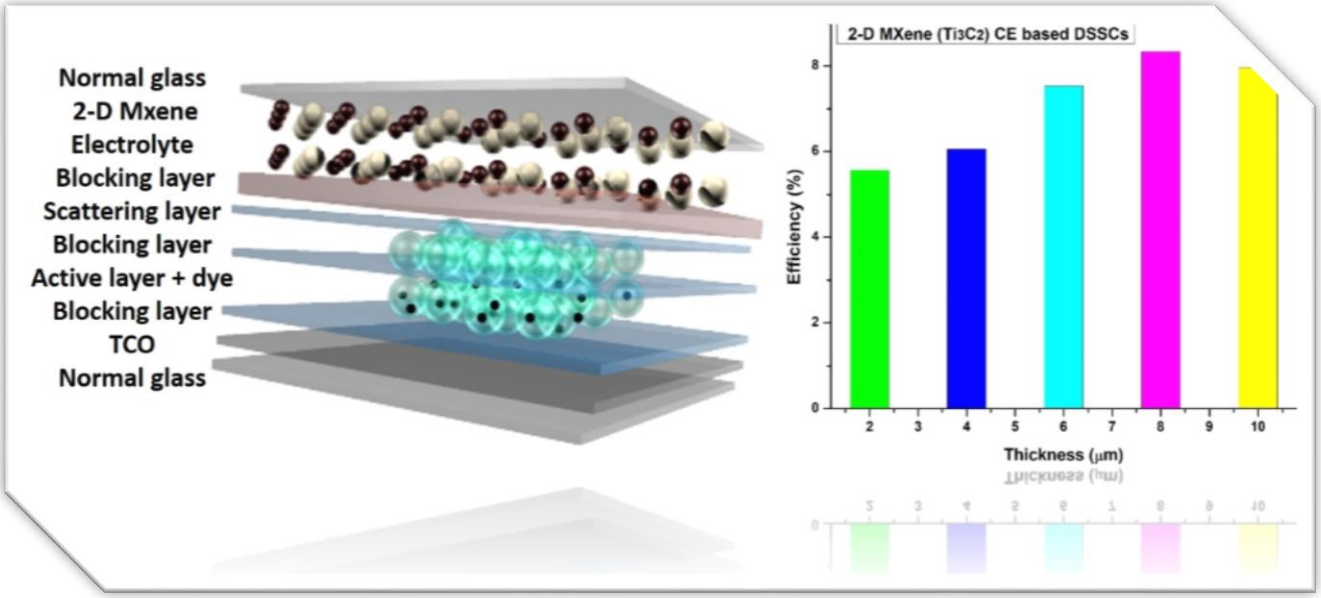

Nomenclature

Voc = open circuit voltage

Isc = short circuit current

TCO = transparent conducting oxide

Pt = platinum

DSSC = dye sensitized solar cell

CE = CE

SEM = scanning electron microscopy

XRD = X-ray diffraction

CV = cyclic voltammetry

EIS = electron/electrochemical impedance spectroscopy

IV curve = current-voltage curve

FTO = fluorine doped tin oxide

PET = Polyethylene Terephthalate

LUMO = lower unoccupied molecular orbital

SE mode = secondary electron mode

1. Introduction

Global industrialization and modern lifestyle caused an exponential increase in global energy demand which is expected to be doubled by 2050. Currently, most of the energy demand has been met by fossil fuels which are already on the brink of extinction. Another issue with fossil fuels is our immature power generation technologies which cause high CO_2 emissions[1]. Only the power generation sector contributes 75% of CO_2 emissions. These emissions are causing global warming and air pollution. To address this increased use of fossil fuels and extreme climatic changes, scientists and policymakers are focusing on renewable, cleaner, and sustainable sources of energy [2]. Furthermore, huge investments have been made in research and development to increase energy use in the form of electricity. Currently, the share of electricity in the primary energy mix is around 19% which is expected to reach 29% by 2050 [3].

Various renewable, clean, and sustainable energy sources i.e.,solar, wind, nuclear, tidal, geothermal and biomass, etc. have been proposed. Among them, solar energy proved to be the ultimate energy source due to its availability, abundance, and sustainability. Solar energy can be converted into usable heat energy or directly into electricity by using solar photovoltaic (PV) cells. Recently, solar PV attracted a lot of attention due to its high reduction in cost, simplicity,and ease in installation. Solar PVs can be divided into three main generations i.e., (a) 1^{st}-generation solar cells which include mono and polycrystalline solar cells, (b) 2^{nd}-generation solar cells including thin film CdTe, CIGS, etc. based solar cells, and (3) 3^{rd}-generation solar cells which includes organic solar cells, DSSCs, and Perovskites. Among third-generation solar

cells, The technology of DSSCs gained much interest because of its simple and environment-friendly manufacturing, cost-effectiveness, lightweight nature, optimum efficiency, and ability to fabricate flexible modules [4].

The DSSC is essentially a sandwich construct comprised of a photoanode, suitable electrolyte, and CE. The photoanode consists of conducting substrate (most commonly FTO coated rigid glass or SnO_2 coated flexible PET sheets), semiconductor active layer (most commonly nanoscale TiO_2), and any suitable dye sensitizer. On the other hand, the CE consists of the same conducting substrates coated with a suitable catalyst (the most common catalyst is platinum). The iodide/triiodide-based electrolytes have been used commonly to act as an electron shuttle between photoanode and CE. In general, the photoactive dye gets oxidized by the incident photons and the ejected electron has been transferred to semiconductor nano-architecture due to suitable symmetry of LUMO of dye and semi-conductor. The oxidized dye gets reduced by accepting an electron from the electrolyte. The electron travels to the outer circuit through the TCO layer and entered the device through the CE. The oxidized electrolyte gets reduced by accepting external electrons. The catalyst layer at CE is responsible for the efficient regeneration of electrolytes. This regeneration cycle continued until the photons are available [5-6].

The most expensive constituent of the DSSC device is a Pt-based catalyst. Pt is a rare earth metal and its availability is limited which renders its full commercialization potential. Although Pt is considered to be an ideal catalyst and exhibited the highest catalytic activity towards electrolytes, it is prone to photocorrosion due to an acidic environment and loses its activity over time [7]. Various earth-abundant and cost-effective materials such as carbon & its allotropic forms [8-9], metal carbides [10], metal sulfides [11], pure metallic nanoparticles [12], and their nano-architectures have been tried with impressive and promising claims [13-14]. The carbides of

transmission metals have been immensely investigated to replace Pt as a catalyst. In a recent study, Mo-based binary/ternary nanocomposites (Mo_2C and Bi/Mo_2C) have been investigated. The claimed efficiency of Mo_2C and Bi/Mo_2C in mesoporous carbon was 7.29% and 8.06% respectively which is much higher compared to Pt based DSSC (7.29%) [15]. Tungsten carbide [16] and iron carbide [17] have also been tried with efficiencies i.e., 7.01% and 7.35%.

Recently, the metal carbide-based 2-D MXenesi.e., Ti_3C_2gained immense interest due to their biocompatibility, large interlayer spacing, high catalytic activity, environmental flexibility, a large surface area, and thermal& electrical conductivity [18-20]. It has been tried in various applications such as energy storage, energy conversion, supercapacitors, water purification, and anti-microbial applications [21-22]. Although, the material promises a huge set of electronic and catalytic properties, very little knowledge has been published in the field of DSSC as a CE. In a study, 2-D MXene (Ti_3C_2) with CuSe nanoparticles has been investigated in a quantum dot solar cell as a CE. The highest efficiency at optimum concentration was claimed to be 5.12% [23]. Although MXenes have been investigated as CEs in the field of DSSC still the literature is very scarce and very little has been investigated about the effect of various parameters such as precursor being employed, synthesis method, and optimization. In another study, Ti_3C_2 has been investigated as CE in DSSC and Perovskite. The nanoparticles of Ti_3C_2 have been spray coated on FTO glass and sintered at 120^oC. A remarkable efficiency of 9.57% in for DSSC and 7.78% in case of Perovskite have been claimed, heavily outperforming Pt based standard CE in case of DSSC [24]. Recently, heavily oxidized MXene has been employed as a semi-conductor network in perovskite solar cells. The reported efficiency was claimed to be 18.29% which has been attributed to reduced electron-hole recombination, high charge transferability, and compatibility with conducting layer [20].

In this study, we employ Metallo-ceramic MXene as a CE for DSSC due to its high surface area, high amount of exposed catalytic sites, charge transfer properties, and ability to fabricate catalyst layer at relatively lower temperatures as the case with Pt-based catalytic layer. Furthermore, for the first time, we systematically investigated the performance of MXene as a cost-effective TCO-Pt-freeCE catalyst layer for DSSC applications by studying the effect of layer thickness. The objective was to achieve the optimum layer thickness with the highest amount of exposed catalytic sites and optimum length of charge transfer. MXene has been drop cast on normal non-conducting glass and applied as a CE for DSSC. TCO-Pt-based CEs have also been fabricated for comparison purposes. The MXene based CE would prove to be the best replacement to TCO-Pt CE in terms of availability, low annealing temperatures, high surface area, excellent corrosion resistance, and non-toxicity.

2. Experimental:

2.1. Materials:

MAX Phase (Ti_3AlC_2) (supplied by: Y-Carbon Ltd), Ammonium hydrogen difluoride (NH^3HF_2) (Sigma Aldrich), sodium hydroxide (Sigma Aldrich), ethanol (Merck), acetone (Merck), Ruthenium dye (Solaronix), acetonitrile (Sigma Aldrich), TiO_2 coated FTO glass (Solaronix), FTO glass (Solaronix), TCO-Pt CE (Solaronix), sealing film (Solaronix).

2.2. Synthesis of MXene:

2-D MXene has been produced through leaching of MAX-phase. In brief, 2M solution of NH_4HF_2in DI water has been prepared stirred for 1hr at room temperature. Afterward, 1 g of Ti_3AlC_2 was added to the solution dropwise (slow addition due to exothermic reaction) with continuous stirringat 300 rpm. The solution was stirred for 48 h at room temperature.

NaOHsolution in DI water has been used to adjust the pH to 6. The pH-adjusted solution was filtered and rinsed using DI water. The achieved multi-layered $Ti_3C_2T_x$was then suspended in ethanol and sonicated for 1 hour using an ultrasonic probe sonicator (FS-1200N). The power of sonicator was set to 60% and on/off time of 7/3 second to obtain delaminated MXene (d-$Ti_3C_2T_x$). The as-synthesized MXene has been dried oven overnight in vacuum condition.

2.3. Fabrication of CE:

The dried delaminated MXene powder has been suspended in ethanol (concentration 25mg/ml) and drop-cast on normal glass. The temperature of the glass has been set to 60^{o}C using a hot plate throughout the drop-casting process. The drop rate was set to 10 drops a min. The active area was 1x1cm, the rest of the glass has been covered by masking tape. 5ml of suspension has been drop cast. After that, the casted glass has been heated to 120^{o}C for 2hrs to achieve a well-sintered layer. The same process has been repeated to prepare all the specimens. TCO-Pt reference electrode has been used for comparison purposes and to achieve maximum achievable performance.

2.4. Fabrication of DSSC:

The TiO_2 coated FTO glass has been purchased from solaronix and used as received. The TiO_2 coated FTO glass has been dipped in Ruthenium-based dye (triisothiocyanato-[2,2’:6’,6’’-terpyridyl-4,4’,4’’-tricarboxykato] ruthenium[II] tris[tetra-butyl-ammonium] with ethanol overnight and rinsed with DI water thoroughly. The already fabricated CEs were placed on top of the photoanode separated by polymer sealing film and filled with Iodide/triiodide redox electrolyte (0.5 M LiI, 0.05 M I_2, and 0.1 M 4-tert-butylpyridine in 1:1 isopropyl alcohol) through pin holes on the CEs. The pin holes were sealed with the melt glue gun and the film was

sealed by heating the polymer film through a hot air blower. At least five specimens have been prepared for each testing. Pre-fabricated TCO-Pt counter has been used as reference CE to avoid human errors and to achieve the highest possible conversion efficiency for accurate comparisons. The complete process has also been illustrated in figure 1.

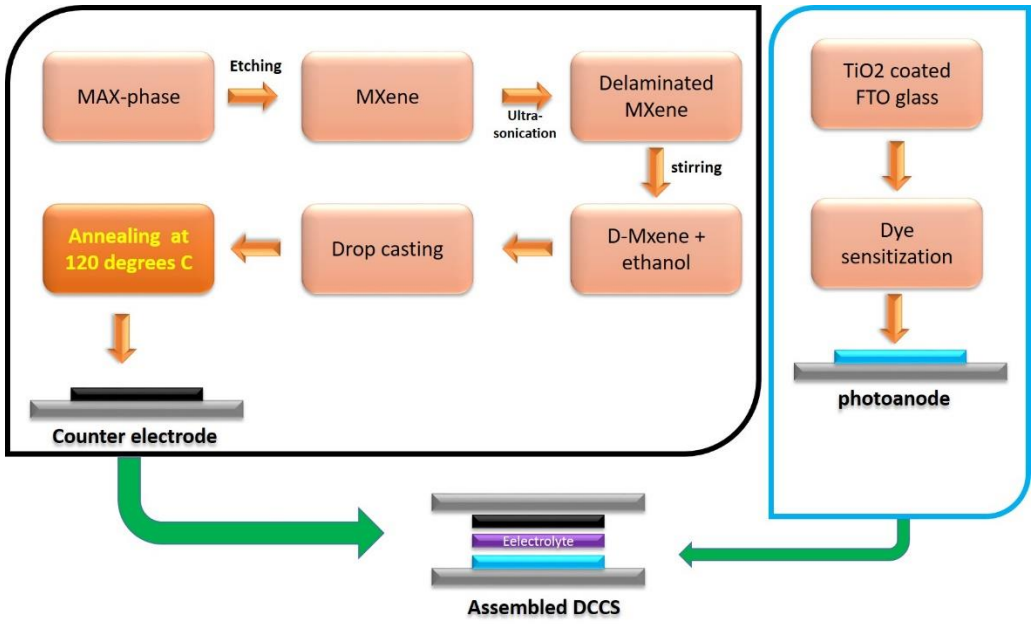

Figure 1: Schematic illustration of an experimental process

2.5. Characterization:

The surface morphology and particle size have been estimated using SEM (model: tescon Mira). The operating power was 5KV and the SEM has been used inSE mode. The distance between the stage to the gun was adjusted to 5mm. XRD (Bruker D8 discover) has been employed for phase identification. The anode material was copper and the machine has been operated between °2θ. 5.0131 and °2θ. 89.9551 with Step Size (°2θ. 0.0260). The catalytic activity and stability have been examined using CV (Autolab potentiostat).The configuration of the electrochemical cell (operated at potential ranges of -1.0 to 1.0V and scan rate was optimized to 20mVs^{-1}) for CV includes working electrode, CE (Pt wire), and Ag/AgCl as reference electrode. The electrolyte

has been prepared using iodide/triiodide ions (detail is given above. To measure electron kinetics in the DSSC, i.e., overall resistance for the electron to travel from layer to layer, EIS has been utilized. The operating frequency range of the potentiostat was set to 0.1-1MHz. An ultrasonic method using a portable Alcometer (model S) has been used to measure coating thickness. Finally, a sun simulator has been employed to measure I-V characteristics, V_{oc} and J_{sc}. The IVT 300 series solar simulator uses a 1600W Xenon lamp (SAN-EI electric Co., Ltd).A certified golden solar cell (Amorphous Silicon solar cell) has been used to calibrate the machine before testing. Standard Amorphous Si solar cell has beenselected as it showed minimum mismatch and assumed to be similar in action spectra with DSSCs. The calculated mismatch was approximately 3.7%, which was adjusted in machine parameters as a mismatch factorfor proper measurements.

3. Results and Discussion

SEM and XRD have been performed to examine surface morphology and composition respectively. Figure 2(a) shows SEM micrographs of as-synthesized MXene. The delamination is evident from figure 2(a). The thickness of the delaminated flake is less than 100nm whereas; the other dimensions are in micro-scale. Figure 2(b) shows the XRD pattern of Ti_3C_2. The peaks being identified near 2theta values of 10, 20, 40, and 60 represent 2-D MXene Ti_3C_2 with corresponding indices i.e., (002), (006), (002), and (110) respectively.

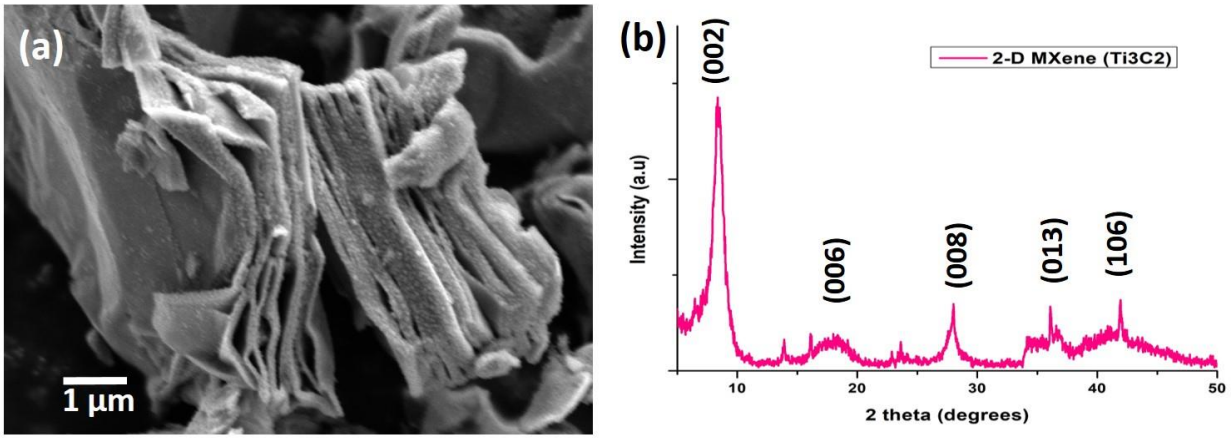

Figure 2: (a,b) SEM micrographs of delaminated 2-D MXene (Ti_3C_2), (c) XRD pattern and (d) FTIR pattern

CV under three electron configurations has been conducted for the catalytic activity of the specimens. The same electrolyte as described in the experimental section has been used with Ag/AgCl as reference electrode and Pt wire as a CE. The electrolyte has been bubbled with argon gas for 5 minutes before testing. Figure 3(a) shows the CV curves of the specimens under investigation. Redox peaks for each curve are observed in figure 3(a), suggesting a reduction of I_3^- to I^- (left side) and oxidation of I^- to I_3^- (right side). The reduction and oxidation reactions are explained through Eq 1 and 2 respectively.

$$I_3^- + 2e^- \rightleftharpoons 3I^- \text{ ----- (eq 1)}$$

$$3I_2 + 2e^- \rightleftharpoons 2I_3^- \text{ --------- (eq 2)}$$

It is well known that the performance of DSSC is directly related to the electrocatalytic activity of catalyst towards the reduction of I_3^-. High cathodic current density suggests faster kinetics of the electrocatalytic process. It has been observed that with the increase in thickness, the catalytic activity increases as can be seen in figure 3. The redox peaks showing a positive shift towards

high current density. The highest catalytic activity towards iodide/triiodide redox shuffle has been observed for specimens with 8µm thickness. This can be correlated with the increase in available catalytic sites and the high catalytic activity of Ti_3C_2 towards iodide/triiodide-based electrolytes. The CV of TCO-Pt-based CE has also been conducted for comparison. The redox peaks of TCO-Pt-based CE show lower current densities compared to the highest performing Ti_3C_2 based CE with optimum thickness. The bare TCO glass-based CE did not show any or negligible redox peaks.

A multi-cycle successive scanning CV measurement has been conducted to further examine the electrochemical stability of prepared Mxene CE in the iodide-based electrolyte. Best performing CE i.e., Mxene with 8µm thickness has been selected for this study and tested till the 40^{th} cycle at $20mVs^{-1}$ scan rate. Figure 3(b) shows the electrochemical stability. No change in the shape of the CV curve has been observed. Further, very few variations in peak current density suggest good stability of the catalyst in the electrolyte.

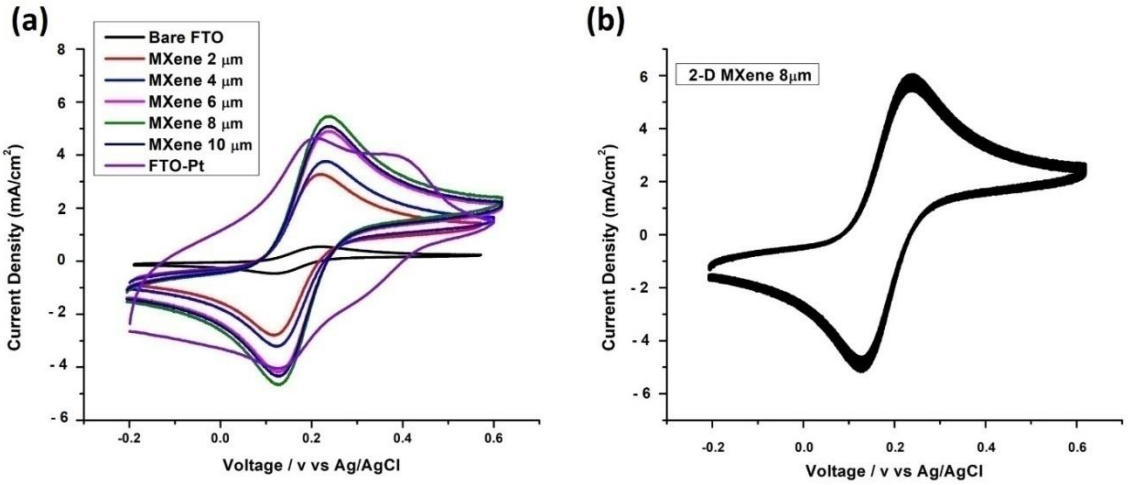

Figure 3:(a) voltammograms of specimens and (b) CV curve of 40 cycle successive scans at $20mVs^{-1}$

Figure 4 shows the EIS pattern of the specimens under investigation. EIS is a powerful tool to understand electron kinetics and the overall resistance in the electronic path. Dummy cell consists of two identical electrodes separated by sacked filter paper with electrolyte has been used for EIS studies. The equivalent circuit has also been presented in figure 3. Refereeing to the first semicircle, a negative shift for Rs(series resistance) and Rct(charge transfer resistance) have been observed with an increase in layer thickness. The second semicircle represents the Warburg diffusion resistance of iodide/triiodide-based electrolytes. The Rs values of the specimens ranging from $1.30\Omega cm^{-2}$ – $3.26\ \Omega.cm^{-2}$ which shows good surface adhesion of all the specimens. Further, the lowest Rct value of approximately $1.81\Omega.cm^{-2}$ has been observed for Mxene specimens of 8 µm thickness. This is due to the favorable electronic path and interaction of electrolytes with catalytic sites due to optimum surface area. Further increase in layer thickness leads to degradation ofelectronic transfer properties which can be explained based on the increased electronic travel distance. It should be mentioned here that the EIS curves are draws for sandwich dummy cells which showed double values for Rct due to two electrodes.

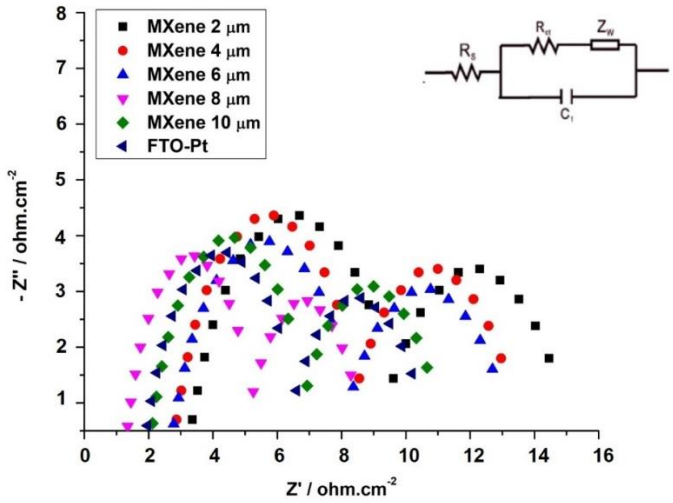

Figure 4: EIS pattern of specimens under investigation

Figure 5(a) shows the I-V curves of the specimens and details of parameters have been provided in table 1. The TCO-Pt free Ti_3C_2 CE-based DSSCs with 2µm thickness exhibited a conversion efficiency of 5.61% with values of V_{oc} and I_{sc} as 0.721V and 11.14mA/cm^2 respectively. The conversion efficiency increases with an increase in layer thickness.

By increasing the thickness, the surface area increases. As the layer is porous, the amount of exposed edge planes and surface in the layer increases by increased thickness.This increase in thickness favors the reduction rate of triiodide ions and causes a reduction in R_{ct} value. The reduction in R_{ct} value corresponds to enhanced current density and fill factorwhich translates into higher photoconversion efficiency. However, further increment in thickness leads to deterioration of device properties i.e., I_{sc}, FF, and conversion efficiency. This is due to increased transport length for I^{3-} transfer. This long traveling path leads to areduction in overall performance. This phenomenon has been illustrated by a schematic diagram as shown in figure 5(b).

The maximum efficiency of 8.68% with V_{oc} and I_{sc} values of 0.758V and 17.10mA/cm^2 respectively has been exhibited by Ti_3C_2 CE-based DSSCs with 8µm layer thickness. This is due to the high availability of catalytic sites, excellent electrical conductivity, and high catalytic activity which corresponds to CV and EIS results shown in Figures 3&4. Further increase in thickness leads to a reduction in conversion efficiency which can be co-related with CV and EIS results for higher charge traveling path. The high charge traveling path leads to the creation of electron trapping sites that resist the charge transfer. For comparison purposes, TCO-Pt CE-based DSSC specimens have also been tested for their overall performance. The reference TCO-Pt CE-based DSSC exhibited the overall conversion efficiency of 8.33% which is 4.03% lower compared to the highest performing TCO-Pt free Ti_3C_2 based CE with 8µm thickness.

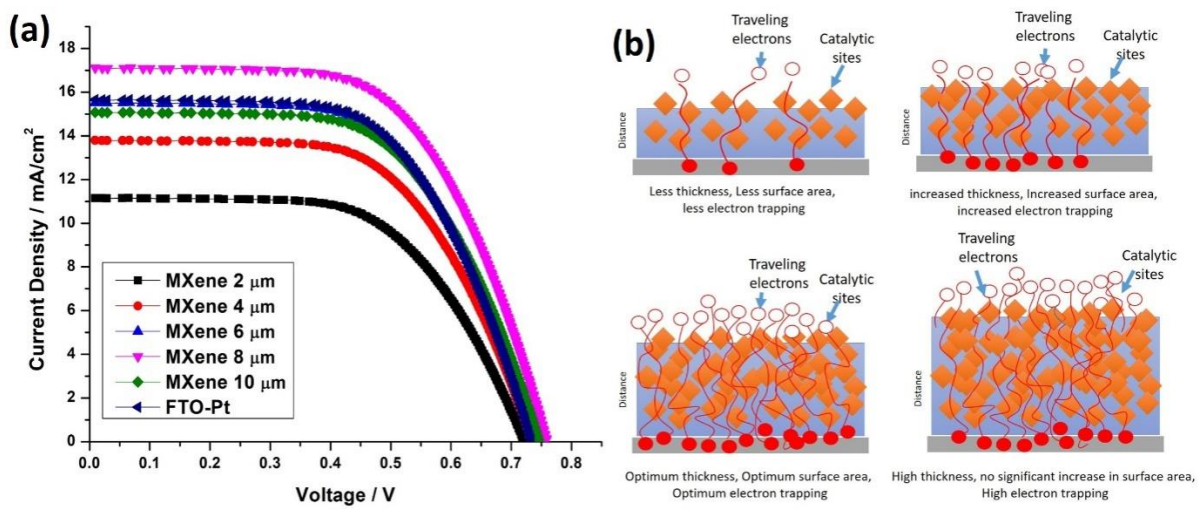

Figure 5:(a) I-V characterization of specimens under investigation and (b) schematic illustration of the mechanism

Table 1: Detailed summary of I-V parameters of specimens under investigation

Sr. No.	Specimen ID	Thickness (µm)	V_{oc} (V)	I_{sc} (mA/cm^2)	FF (%)	EFF (%)
1	MXene CE based DSSC	2	0.721	11.14	70	5.61
2	MXene CE based DSSC	4	0.733	13.79	72	6.23
3	MXene CE based DSSC	6	0.739	15.50	72	7.74
4	MXene CE based DSSC	8	0.758	17.10	73	**8.68**
5	MXene CE based DSSC	10	0.745	15.07	70	8.02
6	TCO-Pt CE based DSSC	--	0.733	15.65	73	**8.33**

Minimal to no noticeable change in the value of Voc has been detected. This is because the Voc is related to the Fermi level of semi-conductor being employed in photoanode. As the

photoanodes throughout the investigation were the same, no marked variation in Voc has been observed.

4. Conclusions

In this study, delaminated 2-D MXene (Ti_3C_2) flakes have been investigated as potential TCO-Pt-free CEs for DSSC technology. Furthermore, the thickness has been optimized for maximum overall performance. SEM and XRD have been employed to examine surface morphology and compositional analysis respectively. FTIR has been employed to examine unsaturated redox functionalities. CV and EIS have been utilized to investigate catalytic performance and overall electronic resistance respectively. I-V curves, V_{oc}, I_{sc}, and conversion efficiency have been measured using a solar simulator. The TCO-Pt free MXene based CE exhibited with 8µm layer thickness exhibited 8.68% conversion efficiency outperforming the standard Pt-TCO-based CE by 4.03%. The high conversion efficiency Ti_3C_2 CE-based DSSCs can be co-related with high surface area, good catalytic activity, and high charge transferability. The proposed TCO-Pt-free CE material is highly cost-effective and requires moderate sintering temperatures. The material can be a potential replacement for both TCO and Pt in the DSSC device.

Acknowledgments

The authors acknowledge the financial assistance of Ministry of Higher Education, Malaysia under Fundamental Research Grant Scheme (FRGS) (FRGS/1/2020/STG05/SYUC/02/1) for carrying out this research.The authors also thank the technical and financial assistance of UM Power Energy Dedicated Advanced Centre (UMPEDAC) and the Higher Institution Centre of Excellence (HICoE) Program Research Grant, UMPEDAC - 2018 (MOHE HICOE -

UMPEDAC), Ministry of Education Malaysia, TOP100UMPEDAC, RU005-2015, University of Malaya.

Data Availability: Data will be made available on request.

References:

[1] V. Litvinenko, The role of hydrocarbons in the global energy agenda: The focus on liquefied natural gas, Resources 9 (5) (2020) 59.
[2] R.M. Elavarasan, G. Shafiullah, S. Padmanaban, N.M. Kumar, A. Annam, A.M. Vetrichelvan, L. Mihet-Popa, J.B. Holm-Nielsen, A comprehensive review on renewable energy development, challenges, and policies of leading Indian states with an international perspective, IEEE Access 8 (2020) 74432-74457.
[3] McKinsey, Global energy perspective 2019: reference case, in: C. Tryggestad (Ed.), Energy Insights, 2019.
[4] M.S. Ahmad, N. Abd Rahim, S. Mehmood, A.D. Khan, Effect of WS2 nano-sheets on the catalytic activity of polyaniline nano-rods based counter electrode for dye sensitized solar cell, Physica E: Low-dimensional Systems and Nanostructures 126 (2021) 114466.
[5] M.S. Ahmad, A.K. Pandey, N. Abd Rahim, Effect of Nanodiamonds on the Optoelectronic Properties of TiO $$ _ {2} $$2 Photoanode in Dye-Sensitized Solar Cell, Arabian Journal for Science and Engineering 43 (7) (2018) 3515-3519.
[6] A.K. Pandey, M.S. Ahmad, M. Alizadeh, N. Abd Rahim, Improved electron density through hetero-junction binary sensitized TiO_2/CdTe/D719 system as photoanode for dye sensitized solar cell, Physica E: Low-dimensional Systems and Nanostructures 101 (2018) 139-143.
[7] U. Ahmed, M. Alizadeh, N.A. Rahim, S. Shahabuddin, M.S. Ahmed, A. Pandey, A comprehensive review on counter electrodes for dye sensitized solar cells: A special focus on Pt-TCO free counter electrodes, Solar Energy 174 (2018) 1097-1125.
[8] K.D.M.S.P.K. Kumarasinghe, G.R.A. Kumara, R.M.G. Rajapakse, D.N. Liyanage, K. Tennakone, Activated coconut shell charcoal based counter electrode for dye-sensitized solar cells, Organic Electronics 71 (2019) 93-97.
[9] K. Wu, L. Chen, C. Duan, J. Gao, M. Wu, Effect of ion doping on catalytic activity of MWCNT-polyaniline counter electrodes in dye-sensitized solar cells, Materials & Design 104 (2016) 298-302.
[10] L. Chen, W. Chen, E. Wang, Graphene with cobalt oxide and tungsten carbide as a low-cost counter electrode catalyst applied in Pt-free dye-sensitized solar cells, Journal of Power Sources 380 (2018) 18-25.
[11] D. Cao, X. Li, X. Yu, N. Cheng, P. Yang, B. Mi, Z. Gao, Low-Cost and Extra-Simple Preparation of Porous NiS2 Counter Electrode for High-Efficiency Dye-Sensitized Solar Cells, physica status solidi (a) 217 (2) (2020) 1900724.
[12] S. Gullace, F. Nastasi, F. Puntoriero, S. Trusso, G. Calogero, A platinum-free nanostructured gold counter electrode for DSSCs prepared by pulsed laser ablation, Applied Surface Science 506 (2020) 144690.
[13] M.S. Ahmad, A.K. Pandey, N. Abd Rahim, V.V. Tyagi, Pt-TCO free sn-ag-cu ternary alloy as cost effective counter electrode layer for dye sensitized solar cell, Optik 206 (2020) 164317.
[14] H. Fayaz, M.S. Ahmad, A.K. Pandey, N.A. Rahim, V.V. Tyagi, A Novel nanodiamond/Zinc nanocomposite as potential counter electrode for flexible dye sensitized solar cell, Solar Energy 197 (2020) 1-5.

[15] S. Yun, Y. Hou, C. Wang, Y. Zhang, X. Zhou, Mo2C-based binary and ternary nanocomposites as high-efficiency counter electrodes for dye-sensitized solar cells, Ceramics International 45 (12) (2019) 15589-15595.
[16] J.S. Jang, D.J. Ham, E. Ramasamy, J. Lee, J.S. Lee, Platinum-free tungsten carbides as an efficient counter electrode for dye sensitized solar cells, Chemical Communications 46 (45) (2010) 8600-8602.
[17] H. Xu, C. Zhang, Z. Wang, S. Pang, X. Zhou, Z. Zhang, G. Cui, Nitrogen-doped carbon and iron carbide nanocomposites as cost-effective counter electrodes of dye-sensitized solar cells, Journal of Materials Chemistry A 2 (13) (2014) 4676-4681.
[18] N. Shpigel, F. Malchik, M.D. Levi, B. Gavriel, G. Bergman, S. Tirosh, N. Leifer, G. Goobes, R. Cohen, M. Weitman, New aqueous energy storage devices comprising graphite cathodes, MXene anodes and concentrated sulfuric acid solutions, Energy Storage Materials (2020).
[19] B. Anasori, M.R. Lukatskaya, Y. Gogotsi, 2D metal carbides and nitrides (MXenes) for energy storage, Nature Reviews Materials 2 (2) (2017) 1-17.
[20] S. Uzun, M. Han, C.J. Strobel, K. Hantanasirisakul, A. Goad, G. Dion, Y. Gogotsi, Highly conductive and scalable Ti3C2Tx-coated fabrics for efficient electromagnetic interference shielding, Carbon 174 (2021) 382-389.
[21] B.-M. Jun, S. Kim, J. Heo, C.M. Park, N. Her, M. Jang, Y. Huang, J. Han, Y. Yoon, Review of MXenes as new nanomaterials for energy storage/delivery and selected environmental applications, Nano Research 12 (3) (2019) 471-487.
[22] N.E. Mansoor, L.A.D. Aldana, C.E. Shuck, Y. Gogotsi, T.E. Lister, D. Estrada, Removal and Recovery of Ammonia from Wastewater using Ti $ _3 $ C $ _2 $ T $ _x $ MXenes in Flow Electrode Capacitive Deionization, arXiv preprint arXiv:2007.02853 (2020).
[23] Y. Chen, D. Wang, Y. Lin, X. Zou, T. Xie, In suit growth of CuSe nanoparticles on MXene (Ti3C2) nanosheets as an efficient counter electrode for quantum dot-sensitized solar cells, Electrochimica Acta 316 (2019) 248-256.
[24] J.y. Ma, M. Sun, Y.a. Zhu, H. Zhou, K. Wu, J. Xiao, M. Wu, Highly Effective 2D Layer Structured Titanium Carbide Electrode for Dye-Sensitized and Perovskite Solar Cells, ChemElectroChem 7 (5) (2020) 1149-1154.